Tetrametallic Alkylidyne Clusters: $(\mu\text{-H})Ru_4(\mu_4\text{-}\eta^2\text{-COMe})(CO)_{12}$, $(\mu\text{-H})Ru_4(\mu_3\text{-COMe})(CO)_9\{(PPh_2)_3CH\}$, and $(\mu\text{-H})Ru_3Fe(\mu_4\text{-}\eta^2\text{-CX})(CO)_{12}$ (X = OMe, NMe_2). Crystal Structures of $(\mu\text{-H})Ru_4(\mu_4\text{-}\eta^2\text{-COMe})(CO)_{12}$ and $(\mu\text{-H})Ru_3Fe(\mu_4\text{-}\eta^2\text{-COMe})(CO)_{12}$†

Melvyn Rowen Churchill,* Charles H. Lake, Fred J. Safarowic, Derrick S. Parfitt, Leigh R. Nevinger, and Jerome B. Keister*

Department of Chemistry, State University of New York, University at Buffalo, Buffalo, New York 14214

Received June 10, 1992

The clusters $(\mu\text{-H})Ru_3M(\mu_4\text{-}\eta^2\text{-COMe})(CO)_{12}$ (M = Ru, Fe) have been prepared and characterized by single-crystal X-ray diffraction techniques. Also prepared were $(\mu\text{-H})Ru_3Fe(\mu_4\text{-}\eta^2\text{-CNMe}_2)(CO)_{12}$ (low yield) and $(\mu\text{-H})Ru_4(\mu_3\text{-COMe})(CO)_9\{(PPh_2)_3CH\}$, both characterized by spectroscopic methods. The isomorphous complexes $(\mu\text{-H})Ru_3M(\mu_4\text{-}\eta^2\text{-COMe})(CO)_{12}$ (M = Ru, Fe) crystallize in the centrosymmetric space group $P2_1/c$. Unit cell parameters for the tetraruthenium complex are a = 9.277 (2) Å, b = 9.441 (1) Å, c = 25.041 (3) Å, β = 92.53 (1)°, V = 2191.2 (5) Å^3, and Z = 4; for the triruthenium–iron complex they are a = 9.188 (1) Å, b = 9.433 (1) Å, c = 24.820 (3) Å, β = 91.50 (1)°, V = 2150.5 (4) Å^3, and Z = 4. The complexes each contain a tetranuclear cluster of metal atoms in a butterfly configuration. The iron atom in the Ru_3Fe species occupies a "wing-tip" position. Each complex contains three terminal carbonyl ligands linked to each metal atom, a μ-hydride ligand bridging the "bridgehead" metal atoms, and a complex μ_4-η^2-COMe ligand in which the alkylidyne carbon atom interacts with all four metal atoms and the oxygen atom is linked to one wing-tip ruthenium atom.

Introduction

Tetrametallic clusters containing the alkylidyne fragment pose interesting questions concerning structure, bonding and chemical reactivity. Three structural types have been identified: a tetrahedral M_4 unit with a μ_3-CX ligand (type I), a butterfly $M_4(\mu_4\text{-}\eta^1\text{-CX})$ structure (type

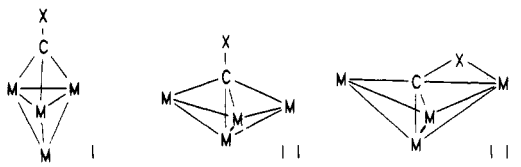

II), and a butterfly $M_4(\mu_4\text{-}\eta^2\text{-CX})$ structure (type III) for X = H, OMe, and NMe_2.[1] The reasons for the structural preferences are not clearly understood, and the reactivity of the alkylidyne ligand in type II and III environments is largely unexplored. The largest number of homometallic clusters of these classes are tetrairon clusters. Examples include $(\mu\text{-H})Fe_4(\mu_4\text{-}\eta^2\text{-COMe})(CO)_{12}$ (type III),[2] [PPN][$Fe_4(\mu_4$-CC(O)R)$(CO)_{12}$] (R = OMe, Me, Bz) (type II),[3] and [PPN][$Fe_4(\mu_3$-CR)$(CO)_{12}$] (type I).[4]

Type III iron butterfly clusters have been proposed as models for some of the chemisorbed intermediates involved in CO reduction to methane and other hydrocarbons over group 8 metal catalysts.[5] Protonation of $(\mu\text{-H})Fe_4(\mu_4\text{-}\eta^2$-COR$)(CO)_{12}$, R = H or Me, generates methane, derived by CO reduction.[2] Protonation of $[Ru_4(CO)_{13}]^{2-}$ produced less methane than the Fe_4 analog, and no Ru_4 butterfly carbides or methynes were detected.[6] However, both metallic Ru and Fe are excellent CO reduction catalysts. Comparative studies of group 8 tetrametallic clusters containing alkylidyne ligands may provide insight into the influence of the metal cluster core upon CO reduction via alkylidyne intermediates.

Ruthenium tetrametallic alkylidynes are rarer than those of iron. Adams et al. prepared $(\mu\text{-H})Ru_4(\mu_4\text{-}\eta^2$-$CNMe_2)(CO)_{12}$ by reaction of $(\mu\text{-H})Ru_3(\mu\text{-}CNMe_2)(CO)_{10}$ with $Ru(CO)_5$;[7] the structure of this type III cluster was established by X-ray crystallography. Johnson, Lewis, and co-workers prepared $H_2Ru_4(C)(CO)_{12}$; this cluster exists as two isomers in solution, one of which appears to be $(\mu\text{-H})Ru_4(\mu_4\text{-}\eta^2\text{-CH})(CO)_{12}$.[28]

A larger number of heterometallic M_4(CR) clusters have been prepared, including $Cp_3Co_2MoFe(CO)_5(\mu_4$-CCO_2-*i*-Pr)[8] and $WRu_3(CO)_{11}Cp(\mu_3$-COMe).[9] These clusters may be prepared by addition of metal fragments to trimetallic

† Structural Studies on Ruthenium Carbonyl Hydrides. 17.

(1) For a general review of butterfly clusters see: Sappa, E.; Tiripicchio, A.; Carty, A. J.; Toogood, G. E. *Prog. Inorg. Chem.* 1987, *35*, 437.

(2) (a) Whitmire, K. H.; Shriver, D. F. *J. Am. Chem. Soc.* 1981, *103*, 6754. (b) Whitmire, K.; Shriver, D. F.; Holt, E. M. *J. Chem. Soc., Chem. Commun.* 1980, 780. (c) Dawson, P. A.; Johnson, B. F. G.; Lewis, J.; Raithby, P. R. *J. Chem. Soc., Chem. Commun.* 1980, 781. (d) Holt, E. M.; Whitmire, K.; Shriver, D. F. *J. Organomet. Chem.* 1981, *213*, 125.

(3) (a) Wang, J.; Crespi, A. M.; Sabat, M.; Harris, S. Woodcock, C.; Shriver, D. *Inorg. Chem.* 1989, *28*, 697. (b) Bogdan, P. L.; Woodcock, C.; Shriver, D. F. *Organometallics* 1987, *6*, 1377. (c) Davis, J. H.; Beno, M. A.; Williams, J. H.; Zimmie, J.; Tachikawa, M.; Muetterties, E. L. *Proc. Natl. Acad. Sci. U.S.A.* 1981, *78*, 668. (d) Bradley, J. S.; Harris, S.; Newsam, J. M.; Hill, E. W.; Leta, S.; Modrick, M. A. *Organometallics* 1987, *6*, 2060.

(4) (a) Holt, E. M.; Whitmire, K. H.; Shriver, D. F. *J. Am. Chem. Soc.* 1982, *104*, 5621. (b) Bogdan, P. L.; Woodcock, C.; Shriver, D. F. *Organometallics* 1987, *6*, 1377.

(5) Drezdon, M. A.; Whitmire, K. H.; Bhattacharya, A. A.; Hsu, W.-L.; Nagel, C. C.; Shore, S. G.; Shriver, D. F. *J. Am. Chem. Soc.* 1982, *104*, 5630.

(6) Muetterties, E. L.; Stein, J. *Chem. Rev.* 1979, *79*, 479.

(7) Adams, R. D.; Babin, J. E.; Tanner, J. *Organometallics* 1988, *7*, 765.

(8) Mlekuz, M.; Bougeard, P.; Sayer, B. G.; Faggiani, R.; Lock, C. J. L.; McGlinchey, M. J.; Jaouen, G. *Organometallics* 1985, *4*, 2046.

0276-7333/93/2312-0671$04.00/0 © 1993 American Chemical Society

alkylidyne clusters. Stone has very successfully exploited the reactions of monometallic alkylidynes with unsaturated metal complexes to prepare mixed-metal alkylidynes, e.g. $Os_3W(\mu_3\text{-CTol})(CO)_{11}Cp$.[10]

Previous work by Adams,[7] Chi,[9] and McGlinchey[8] suggested that it might be possible to synthesize a large class of tetraruthenium and mixed-metal alkylidynes by addition of group 8 metal fragments to $(\mu\text{-H})Ru_3(\mu\text{-CX})(CO)_{10}$ (X = OMe, NMe_2) or $(\mu\text{-H})_3Ru_3(\mu_3\text{-CX})(CO)_9$ (X = Ph, Cl, OMe, and others). In this paper we report the syntheses of $(\mu\text{-H})Ru_4(\mu_3\text{-COMe})(CO)_9\{(PPh_2)_3CH\}$, $(\mu\text{-H})Ru_4(\mu_4\text{-}\eta^2\text{-COMe})(CO)_{12}$, $(\mu\text{-H})Ru_3Fe(\mu_4\text{-}\eta^2\text{-COMe})(CO)_{12}$, and $(\mu\text{-H})Ru_3Fe(\mu_4\text{-}\eta^2\text{-CNMe}_2)(CO)_{12}$ and the crystal structures of $(\mu\text{-H})Ru_3M(\mu_4\text{-}\eta^2\text{-COMe})(CO)_{12}$, M = Ru and Fe.

Experimental Section

$(\mu\text{-H})Ru_3(\mu\text{-COMe})(CO)_{10}$[11] and $(\mu\text{-H})_3Ru_3(\mu_3\text{-COMe})(CO)_7\{(PPh_2)_2CHPPh_2\}$[12] were prepared by previously reported methods. $Ru(CO)_5$ and $Ru(CO)_4(C_2H_4)$ were prepared as stock cyclohexane solutions by photolysis of $Ru_3(CO)_{12}$ under CO or ethylene atmospheres using Pyrex-filtered UV light.[13] ^1H and ^{13}C NMR spectra were recorded on Varian Gemini 300 or VXR-400 Fourier transform spectrometers, and ^{31}P NMR spectra were recorded on the VXR-400 instrument, with chemical shifts measured relative to orthophosphoric acid. Chromium(III) acetylacetonate (0.02 M) was added as a relaxation agent for the ^{13}C NMR spectra. Line shapes of exchange-broadened spectra were compared with line shapes calculated by using DMR3[15] for estimation of the rate constants for fluxionality. Infrared spectra of cyclohexane solutions were recorded on a Beckman 4250 spectrophotometer and were referenced with the 2138.5-cm^{-1} absorption of cyclohexane. Mass spectra were recorded on a VG 70-SE mass spectrometer, and fragment compositions were verified by comparison of experimental and MSCALC-calculated[14] isotope distributions. Elemental analyses were performed by Galbraith Laboratories.

Reaction of $(\mu\text{-H})Ru_3(\mu\text{-COMe})(CO)_{10}$ with $Ru(CO)_5$. A solution of $(\mu\text{-H})Ru_3(\mu\text{-COMe})(CO)_{10}$ (100 mg, 0.159 mmol) in 30 mL of cyclohexane was heated at 70 °C in a 100-mL Schlenk flask under a nitrogen atmosphere. To this were added three 10-mL aliquots of a cyclohexane solution of $Ru(CO)_5$ (113 mg, 0.470 mmol) over a 1-h period. After complete addition the mixture was stirred at 70 °C for an additional 1.5 h. The solvent was removed by vacuum transfer leaving an orange residue. The residue was dissolved in a minimum amount of methylene chloride, leaving undissolved an orange solid, $Ru_3(CO)_{12}$ (29 mg). Preparative TLC (silica gel, cyclohexane/dichloromethane, 3:1 v/v) of the solution yielded the following bands in order of elution: orange $Ru_3(CO)_{12}$ (35 mg), yellow $(\mu\text{-H})Ru_3(\mu\text{-COMe})(CO)_{10}$ (68 mg, 68%), and orange $(\mu\text{-H})Ru_4(\mu_4\text{-}\eta^2\text{-COMe})(CO)_{12}$ (24 mg, 19%, 60% based upon consumed starting material).

Data for $(\mu\text{-H})Ru_4(\mu_4\text{-}\eta^2\text{-COMe})(CO)_{12}$. IR ($C_6H_{12}$): 2084 w, 2062 vs, 2055 vs, 2041 w, 2030 w, 2020 s, 2010 m, 1987 w, and 1978 w cm^{-1}. ^1H NMR ($CDCl_3$, 25 °C): 3.81 (s, 3 H, Me) and −21.76 (s, 1 H, RuHRu) ppm. ^{13}C NMR ($CDCl_3$, 25 °C): 280.8 (1 C), 201.3 (2 C), 195.6 (br, 6 C), 191.6 (4 C), 78.1 (1 C, Me) ppm. ^{13}C NMR ($CDCl_3$, −50 °C): 280.8 (1 C), 201.1 (1 C), 199.4 (2 C), 197.9 (1 C), 195.9 (2 C), 193.4 (2 C), 190.1 (2 C), 190.0 (2 C) ppm. EI MS: m/z 788 ($^{102}Ru_4$). Anal. Calcd for $C_{14}H_4O_{13}Ru_4$: C, 21.44; H, 0.51. Found: C, 23.35; H, 0.66. The compound is unstable, and recrystallized samples are usually contaminated with the decomposition products $HRu_3(COMe)(CO)_{10}$ and $Ru_3(CO)_{12}$, which crystallize quite readily.

Reaction of $(\mu\text{-H})Ru_3(\mu\text{-COMe})(CO)_{10}$ with $Ru(CO)_4(C_2H_4)$. A solution of $(\mu\text{-H})Ru_3(\mu\text{-COMe})(CO)_{10}$ (100 mg, 0.159 mmol) in 30 mL of cyclohexane was heated at 70 °C in a 100-mL Schlenk flask under a nitrogen atmosphere. A cyclohexane solution (100 mL) of $Ru(CO)_4(C_2H_4)$ (0.469 mmol) was added dropwise over a 45-min period. After complete addition the mixture was stirred at 70 °C for 2 h. The solvent was removed by vacuum transfer and the residue dissolved in a minimal amount of methylene chloride. Preparative TLC (silica gel, cyclohexane/methylene chloride, 3:1 v/v) yielded the following bands in order of elution: orange $Ru_3(CO)_{12}$, 58 mg of $(\mu\text{-H})Ru_3(\mu\text{-COMe})(CO)_{10}$, and 34 mg (27%) of $(\mu\text{-H})Ru_4(\mu_4\text{-}\eta^2\text{-COMe})(CO)_{12}$.

Synthesis of $HRu_3Fe(\mu_4\text{-}\eta^2\text{-COMe})(CO)_{12}$. A solution of $(\mu\text{-H})Ru_3(\mu\text{-COMe})(CO)_{10}$ (200 mg, 0.32 mmol) and $Fe(CO)_5$ (200 mL, 1.96 mmol) in 10 mL of cyclohexane was placed in a 50-mL Schlenk flask equipped with a condenser under a nitrogen atmosphere. The solution was heated to 70 °C for 2 h. The solvent and unreacted $Fe(CO)_5$ were removed by vacuum transfer. The final product was separated on a thin-layer chromatography plate (Kieselgel 60G) using cyclohexane as the eluting solvent. The products in order of appearance were as follows: $H_4Ru_4(CO)_{12}$ (6.5 mg, 4%), $(\mu\text{-H})Ru_3(\mu\text{-COMe})(CO)_{10}$ (125.3 mg, 79%), $(\mu\text{-H})Ru_2Fe(\mu\text{-COMe})(CO)_{10}$ (9.6 mg, 6%), $H_2Ru_4(CO)_{13}$ (7.9 mg, 5%), and $(\mu\text{-H})Ru_4(\mu_4\text{-}\eta^2\text{-COMe})(CO)_{12}$ + $(\mu\text{-H})Ru_3Fe(\mu_4\text{-}\eta^2\text{-COMe})(CO)_{12}$ (9.2 mg, 6%). A second separation yielded a pure sample of $(\mu\text{-H})Ru_3Fe(\mu_4\text{-}\eta^2\text{-COMe})(CO)_{12}$.

Data for $(\mu\text{-H})Ru_3Fe(\mu_4\text{-}\eta^2\text{-COMe})(CO)_{12}$. IR ($C_6H_{12}$): 2096 w, 2076 w, 2056 vs, 2036 m, 2018 m, 2006 m, 1992 w, 1980 vw, and 1964 w cm^{-1}. ^1H NMR ($CDCl_3$): 3.90 (s, 3 H, Me) and −21.94 (s, 1 H, RuHRu) ppm. EI MS: m/e 742 ($^{102}Ru_3$).

Synthesis of $(\mu\text{-H})Ru_3Fe(\mu_4\text{-}\eta^2\text{-CNMe}_2)(CO)_{12}$. $(\mu\text{-H})Ru_3(\mu\text{-CNMe}_2)(CO)_{10}$ (200 mg, 0.312 mmol), $Fe(CO)_5$ (400 mL, 3.92 mmol), and 10 mL of cyclohexane were placed in a 50-mL Schlenk flask, equipped with a condenser and gas inlet tube, under a nitrogen atmosphere. The solution was heated at 70 °C for 1.5 h. All volatile components were then removed by vacuum transfer. Thin-layer chromatography using cyclohexane as the eluting solvent showed the following bands: $H_4Ru_4(CO)_{12}$ (4.5 mg, 2%), $H_2Ru_4(CO)_{13}$ (1.9 mg, 1%), $(\mu\text{-H})Ru_3(\mu\text{-CNMe}_2)(CO)_{10}$ (129.4 mg, 65%), $(\mu\text{-H})Ru_2Fe(\mu\text{-CNMe}_2)(CO)_{10}$ (33.5 mg, 18%), and $(\mu\text{-H})Ru_4(\mu_4\text{-}\eta^2\text{-CNMe}_2)(CO)_{12}$ + $(\mu\text{-H})Ru_3Fe(\mu_4\text{-}\eta^2\text{-CNMe}_2)(CO)_{12}$ (1.9 mg, 1%). A second separation yielded a very small amount of the pure mixed-metal cluster.

Data for $(\mu\text{-H})Ru_3Fe(\mu_4\text{-}\eta^2\text{-CNMe}_2)(CO)_{12}$. IR ($C_6H_{12}$): 2093 w, 2057 s, 2048 s, 2028 m, 2021 m, 2004 s, 1992 m, 1969 w, and 1955 w cm^{-1}. ^1H NMR ($CDCl_3$): 3.15 (s, 6 H) and −22.70 (s, 1 H) ppm. EI MS: m/z 755 ($^{102}Ru_3$).

Synthesis of $(\mu\text{-H})Ru_4(\mu_3\text{-COMe})(CO)_9\{(PPh_2)_3CH\}$. To a solution of $(\mu\text{-H})_3Ru_3(\mu_3\text{-COMe})(CO)_7\{(PPh_2)_2CHPPh_2\}$ (100 mg, 0.0897 mmol) in hexanes (25 mL) was added a solution of $Ru(CO)_4(C_2H_4)$ in hexanes (ca. 8 mM, 30 mL). The solution was stirred at room temperature under a nitrogen atmosphere for 2 days. After evaporation of solvent the solid residue was separated by TLC on silica gel, eluting with dichloromethane–hexanes (40:90 v/v). The products were identified as $Ru_3(CO)_{12}$ (4 mg), $(\mu\text{-H})_3Ru_3(\mu_3\text{-COMe})(CO)_7\{(PPh_2)_2CHPPh_2\}$ (66 mg, 66%), and $(\mu\text{-H})Ru_4(\mu_3\text{-COMe})(CO)_9\{(PPh_2)_3CH\}$ (20 mg, 18%).

(9) Chi, Y.; Chuang, S.-H.; Chen, B.-F.; Peng, S.-M.; Lee, G.-H. *J. Chem. Soc., Dalton Trans.* **1990**, 3033.
(10) Busetto, L.; Green, M.; Hessner, B.; Howard, J. A. K.; Jeffery, J. C.; Stone, F. G. A. *J. Chem. Soc., Dalton Trans.* **1983**, 519.
(11) Keister, J. B.; Payne, M. W.; Muscatella, M. J. *Organometallics* **1983**, *2*, 219.
(12) Churchill, M. R.; Lake, C. H.; Feighery, W. G.; Keister, J. B. *Organometallics* **1991**, *10*, 2384.
(13) Johnson, B. F. G.; Lewis, J.; Twigg, M. V. *J. Organomet. Chem.* **1974**, *67*, C75.
(14) MSCALC is a program written in Quickbasic for calculation of isotope envelopes and comparison with experimental mass spectra. The program was adapted by J.B.K. from the FORTRAN program MASPAN (Andrews, M. A. Ph.D. Dissertation, University of California at Los Angeles, Los Angeles, CA, 1977).
(15) Kleir, D. A.; Binsch, G. DMR3: A Computer Program for the Calculation of Complex Exchange-Broadened NMR Spectra. Modified Version for Spin Systems Exhibiting Magnetic Equivalence of Symmetry. *Quantum Chemistry Program Exchange*; Indiana University: Bloomington, IN, 1970; Program 165. Modified version by D. C. Roe (Du Pont Central Research) for use on a VAX computer and locally modified for use with DI-3000 graphics.

Data for $(\mu\text{-H})Ru_4(\mu_3\text{-COMe})(CO)_9\{(PPh_2)_3CH\}$. IR ($CH_2Cl_2$): 2058 m, 2040 ms, 2028 s, and 1985 s cm^{-1}. ^1H NMR ($CDCl_3$, 25 °C): 8.15 (qd, 1 H, J_{PH} = 7 Hz, J_{HH} = 2 Hz), 7.0 (br m, 30 H), 4.70 (s, 3 H), and −15.95 (qd, 1 H, J_{PH} = 13, J_{HH} = 2 Hz) ppm. $^{31}P\{^1H\}$ NMR ($CDCl_3$, −50 °C): 40.6 (dd, 1 P_A), 35.2 (dd, 1 P_B), 21.4 (dd, 1 P_C) ppm, $J_{AB} \sim J_{AC} \sim J_{BC} \sim$ 24 Hz. ^{31}P NMR (20 °C): 36.1 (t, 1 P), 31.0 (br, 2 P) ppm. $^{13}C\{^1H\}$ NMR ($CDCl_3$, 22 °C): 350.5 (t, 1 C, J_{PC} = 19 Hz), 203.5 (br, 3 C), 201.9 (d, 2 C, J_{PC} = 5 Hz), 200.7 (d, 2 C, J_{PC} = 6 Hz), 200.5 (d, 2 C, J_{PC} = 8 Hz), 127–135 (Ph), and 71.8 (s, 1 C) ppm. FAB MS: m/z 1271 ($^{102}Ru_4$). Anal. Calcd for $Ru_4C_{48}H_{35}O_{10}P_3$: C, 45.43; H, 2.78. Found: C, 44.10, H, 2.70.

Unsuccessful Reactions. Other attempts to make tetraruthenium clusters were made by combining the following pairs of reactants at 25 °C and then slowly heating to 70 °C until one of the reactants was no longer detectable by IR spectroscopy. In most cases greater than 80% of the starting cluster was recovered by preparative TLC.

Reactions attempted: $Ru(CO)_3$(1,5-COD) with $H_3Ru_3(COMe)(CO)_9$, $H_3Ru_3(CCl)(CO)_9$, $H_3Ru_3(CPh)(CO)_9$, $H_3Ru_3(CPh)(CO)_8$(NCMe), $HRu_3(CPh)(CO)_8$(cyclohexadiene), and $HRu_3(CCl)(CO)_8$(cyclohexadiene); $Ru(CO)_5$ with $H_3Ru_3(CCl)(CO)_9$ and $H_3Ru_3(CPh)(CO)_9$; $Ru(CH_2CHCO_2CH_3)(CO)_4$ with $H_3Ru_3(CCl)(CO)_9$, $H_3Ru_3(CPh)(CO)_9$, $HRu_3(CPh)(CO)_8$(cyclohexadiene), $HRu_3(CCl)(CO)_8$(cyclohexadiene), $H_3Ru_3(CPh)(CO)_8$(NCMe), and $H_3Ru_3(CCl)(CO)_8$(NCMe); $Ru(CO)_4(C_2H_4)$ with $H_3Ru_3(CCl)(CO)_9$ and $H_3Ru_3(CPh)(CO)_9$.

Collection of X-ray Data for $(\mu\text{-H})Ru_4(\mu_4\text{-}\eta^2\text{-COMe})(CO)_{12}$. A crystal of $(\mu\text{-H})Ru_4(\mu_4\text{-}\eta^2\text{-COMe})(CO)_{12}$ (0.3 mm × 0.25 mm × 0.25 mm) was sealed into a 0.3-mm-diameter thin-walled capillary. It was then mounted and aligned on a Siemens R3m/V single-crystal diffractometer. One hemisphere of data was collected by a coupled 2θ–θ scan (Mo Kα, 2θ = 5°–45°). A total of 6160 reflections were collected and were merged into a unique set of 2873 reflections (R_{int} = 1.34%).

Determination of unit cell parameters and data collection was carried out as described previously;[16] details appear in Table I. All data were corrected for absorption, Lorentz, and polarization effects. The complex crystallizes in the monoclinic system ($2/m$ diffraction symmetry). The systematic absence $h0l$ for $l = 2n + 1$ and $0k0$ for $k = 2n + 1$ uniquely define the centrosymmetric space group $P2_1/c$ (No. 14).

Collection of X-ray Data for $(\mu\text{-H})Ru_3Fe(\mu_4\text{-}\eta^2\text{-COMe})(CO)_{12}$. A crystal of $(\mu\text{-H})Ru_3Fe(\mu_4\text{-}\eta^2\text{-COMe})(CO)_{12}$ (0.25 mm × 0.2 mm × 0.2 mm) was selected for the X-ray study. The crystal was mounted, and data were collected in exactly the same manner as for the previous compound. Unit cell and data collection parameters are collected in Table I. A total of 6081 reflections were collected and were merged into a unique data set containing 2832 reflections (R_{int} = 1.47%).

This complex was isomorphous with $(\mu\text{-H})Ru_4(\mu_4\text{-}\eta^2\text{-COMe})(CO)_{12}$ and crystallized in space group $P2_1/c$ (No. 14).

Solution and Refinement of the Crystal Structure of $(\mu\text{-H})Ru_4(\mu_4\text{-}\eta^2\text{-COMe})(CO)_{12}$. All crystallographic calculations were performed on a VAX3100 work station, with use of the Siemens SHELXTL PLUS program set.[17] Analytical scattering factors[18a] for neutral atoms were corrected for both the $\Delta f'$ and the $i\Delta f''$ components of anomalous dispersion.[18b] The structure was solved by the use of direct methods and refined to R = 3.94% (R_w = 3.95%) for all 2873 unique reflections and R = 2.80% (R_w = 3.07%) for those 2283 reflections with $F_o > 6.0\sigma(F_o)$. Hydrogen atoms of the methyl group were placed at calculated positions based on the basis of d(C–H) = 0.96 Å.[19] The bridging hydride ligand was located from a difference-Fourier synthesis, and its positional and isotropic thermal parameters were refined. A secondary extinction correction was included in the final model by refining the paramater χ to a final value of 0.000 27 (4). The final difference-Fourier map showed features in the range of −1.08 to +1.43 e Å^{-3}, with the largest feature being 1.024 Å from Ru(4). Final atomic coordinates are provided in Table II.

Solution and Refinement of the Crystal Structure of $(\mu\text{-H})Ru_3Fe(\mu_4\text{-}\eta^2\text{-COMe})(CO)_{12}$. All crystallographic calculations were performed in the same manner as for the tetraruthenium complex. The structure was solved using direct methods and refined to R = 5.59% (R_w = 4.58%) for all 2832 unique reflections and R = 3.02% (R_w = 3.10%) for those 1910 reflections with $F_o > 6.0\sigma(F_o)$. The bridging hydride ligand was located by difference-Fourier methods, and its parameters were refined. A secondary extinction correction was used in the final model (χ = 0.000 16 (2)). A final difference Fourier map showed features in the range −0.73 to +1.10 eÅ^{-3}, the largest peak being 0.871 Å from Fe(1). [Coupled refinement with Fe(1) and Ru(3) as mixed Fe/Ru atoms showed no evidence for scrambling of the "wing-tip" metal atoms.] Final atomic coordinates are given in Table III.

Results and Discussion

The structures adopted by $M_4(CX)$ clusters may be rationalized according to the skeletal electron pair theory but cannot presently be predicted. Both type I and type II clusters contain 6 skeletal electron pairs and are described as closo, based upon a trigonal bipyramidal framework; type III clusters possess 7 skeletal electron pairs, with the alkylidyne carbon atom treated as an "interstitial" atom in an arachno structure derived from an octahedron. This difficulty in predicting structure is illustrated by the rearrangement of the type I cluster $[Fe_4(\mu_3\text{-COMe})(CO)_{12}]^-$ to the type III cluster $(\mu\text{-H})Fe_4(\mu_4\text{-}\eta^2\text{-COMe})(CO)_{12}$ upon protonation, a reaction involving no change in the total electron count. Shriver has proposed that the type III structure is favored by the presence of strong electron acceptors in the hinge position.[20]

$(\mu\text{-H})Ru_4(\mu_4\text{-}\eta^2\text{-COMe})(CO)_{12}$. The reaction of $Ru(CO)_4(C_2H_4)$ with $(\mu\text{-H})Ru_3(\mu\text{-COMe})(CO)_{10}$ gives $(\mu\text{-H})Ru_4(\mu_4\text{-}\eta^2\text{-COMe})(CO)_{12}$ in fair yield. This cluster was first characterized by IR, ^1H and ^{13}C NMR, and mass spectroscopy. The mass spectrum displays the molecular ion and step-wise loss of CO ligands. The chemical shift of the hydride, −21.76 ppm, is similar to that of $(\mu\text{-H})Ru_4(\mu_4\text{-}\eta^2\text{-CNMe}_2)(CO)_{12}$ (type III). The ^{13}C NMR spectrum (see Experimental Section) also indicates a type III structure. At −50 °C the resonances due to the CO ligands present a 1:2:1:2:2:2:2 pattern consistent with the type III structure and inconsistent with type I or II structures; analogous spectra were reported for $(\mu\text{-H})Fe_4(\mu_4\text{-}\eta^2\text{-CX})(CO)_{12}$, X = O$^-$, OMe, and H.[20] The chemical shift of the methylidyne carbon, 280.8 ppm, could be associated with either a μ_3- or a μ_4-alkylidyne ligand.[21] The carbonyl spectrum displays fluxional behavior at room temperature; the most likely fluxional process involves fast exchange of the coordinated OMe moiety between the two wing tip Ru atoms (averaging together the two single-carbonyl resonances at 201.1 and 197.9 ppm and also averaging together the two-carbonyl resonanes at 193.4 and 190.0 ppm due to carbonyls on the wing-tip Ru atoms), coupled with 3-fold exchange among the three CO ligands on each hinge Ru atom at an intermediate rate (averaging the three two-carbonyl resonances at 199.4, 195.9, and 191.1 ppm).

(16) Churchill, M. R.; Lashewycz, R. A.; Rotella, F. J. *Inorg. Chem.* **1977**, *16*, 265.

(17) (a) Siemens SHELXTL PLUS Manual, 2nd ed. Siemens Analytical Instruments, Madison, WI, 1990. (b) Sheldrick, G. M. SHELXTL PLUS Release 4.1 for Siemens R3m/V crystallographic system. Siemens Analytical Instruments, Madison, WI, 1990.

(18) *International Tables for X-Ray Crystallography*; Kynoch Press: Birmingham, England, 1974: (a) pp 99–101, (b) pp 149–150.

(19) Churchill, M. R. *Inorg. Chem.* **1973**, *12*, 1213.

(20) Horwitz, C. P.; Shriver, D. F. *J. Am. Chem. Soc.* **1985**, *107*, 8147.

(21) For $(\mu\text{-H})Fe_4(\mu_4\text{-}\eta^2\text{-COMe})(CO)_{12}$ the chemical shift of the μ_4-C is 301 ppm,[2,4c] whereas the capped tetrahedral cluster $[Fe_4(\mu_3\text{-COMe})(CO)_{12}]^-$ displays a μ_3-C shift of 361.2 ppm.[4a]

Table I. Experimental Data for the X-ray Diffraction Studies on $(\mu\text{-H})Ru_4(\mu_4\text{-}\eta^2\text{-COMe})(CO)_{12}$ and $(\mu\text{-H})Ru_3Fe(\mu_4\text{-}\eta^2\text{-COMe})(CO)_{12}$

	Ru_4 complex	Ru_3Fe complex
	Crystal Data	
empirical formula	$C_{14}H_4O_{13}Ru_4$	$C_{14}H_4FeO_{13}Ru_3$
cryst size, mm	0.30 × 0.25 × 0.25	0.25 × 0.20 × 0.15
cryst system	monoclinic	monoclinic
space group	$P2_1/c$	$P2_1/c$
a, Å	9.277 (2)	9.188 (1)
b, Å	9.441 (1)	9.433 (1)
c, Å	25.041 (3)	24.820 (3)
β, deg	92.53 (1)	91.50 (1)
V, Å^3	2191.2 (5)	2150.5 (4)
Z	4	4
fw	784.5	739.2
D(calc), Mg/m^3	2.378	2.283
abs coeff, mm^{-1}	2.715	2.751
F(000)	1472	1400
	Data Collection	
diffractometer used	Siemens R3m/V	
radiation (λ, Å)	Mo Kα (0.71073)	
temp, K	298	
monochromator	highly oriented graphite cryst	
2θ range	5.0–45.0°	
scan type	2θ–θ	
scan speed	constant; 2.00°/min in ω	
scan range (ω)	0.55° plus Kα separation	0.50° plus Kα separation
bkgd measmt	stationary cryst and stationary counter at beginning and end of scan, each for 25.0% of tot. scan time	
std reflcns	3 measd every 97 reflcns	
index ranges	$0 \le h \le 10, -10 \le k \le 10, -26 \le l \le 26$	$0 \le h \le 9, -10 \le k \le 10, -26 \le l \le 26$
reflcns collcd	6160	6081
no. of independent reflcns	2873 (R_{int} = 1.34%)	2832 (R_{int} = 1.47%)
no. of obsd reflcns	2283 ($F > 6.0\sigma(F)$)	1910 ($F > 6.0\sigma(F)$)
abs corr	semiempirical	semiempirical
min/max transm	0.2739/0.3609	0.3921/0.4799
	Solution and Refinement	
system used	Siemens SHELXTL PLUS (VMS)	
solution	direct methods	
refinement method	full-matix least squares	
quantity minimized	$\sum w(F_o - F_c)^2$	
extinction corr	χ = 0.000 27 (4)	χ = 0.000 16 (2)
	where $F^* = F[1 + 0.002\chi F^2/\sin(2\theta)]^{-1/4}$	
organic H atoms	riding model, fixed isotropic U	
	(hydride ligands refined)	
weighting scheme	$w^{-1} = \sigma^2(F) + 0.0003F^2$	$w^{-1} = \sigma^2(F) + 0.0005F^2$
no. of params refined	285	285
final R indices (all data), %	R = 3.94, R_w = 3.95	R = 5.59, R_w = 4.58
R indices (6.0σ data), %	R = 2.80, R_w = 3.07	R = 3.02, R_w = 3.10
goodness-of-fit	1.51	1.12
largest and mean Δ/σ	0.002, 0.000	0.003, 0.000
data-to-param ratio	10.1:1	9.9:1
largest diff peak, e Å^{-3}	1.43	1.10
largest diff hole, e Å^{-3}	−1.08	−0.73

Similar fluxional behavior has been noted for $(\mu\text{-H})Fe_4(\mu_4\text{-}\eta^2\text{-CX})(CO)_{12}$, X = OMe and H.[2d,22] The cluster is unstable in solution, decomposing over a period of days at room temperature to $(\mu\text{-H})Ru_3(\mu\text{-COMe})(CO)_{10}$ and $Ru_3(CO)_{12}$.

The molecular structure of $(\mu\text{-H})Ru_4(\mu_4\text{-}\eta^2\text{-COMe})(CO)_{12}$ was definitively established by X-ray crystallography. The unit cell consists of discrete molecular units, which are separated by normal van der Waals distances. There are no anomalously short intermolecular contacts. The labeling of atoms in the molecule is shown in Figure 1. Selected interatomic distances and angles are collected in Tables IV and V.

The tetranuclear ruthenium core has a butterfly configuration with the following bond distances: Ru(1)–Ru(2) = 2.823 (1) Å, Ru(1)–Ru(3) = 2.801 (1) Å, Ru(2)–Ru(3) = 2.786 (1) Å, Ru(1)–Ru(4) = 2.810 (1) Å, and Ru(2)–Ru(4) = 2.820 (1) Å. Intermetallic angles are Ru(2)–Ru(1)–Ru(3) = 59.4 (1)°, Ru(2)–Ru(1)–Ru(4) = 60.1 (1)°, Ru(1)–Ru(2)–Ru(3) = 59.9 (1)°, Ru(1)–Ru(2)–Ru(4) = 59.7 (1)°, Ru(1)–Ru(3)–Ru(2) = 60.7 (1)°, and Ru(1)–Ru(4)–Ru(2) = 60.2 (1)°. The "wing-tip" atoms in the tetraruthenium core (Ru(3) and Ru(4)) do not have equivalent ligand environments. Ru(3) is bonded both to the oxygen atom and the alkylidyne carbon atom of the methoxyalkylidyne ligand whereas Ru(4) is bonded only to the alkylidyne carbon atom. Metal–metal distances between the ruthenium atoms are affected by the method of coordination of the –COMe ligand. The net result is an increase in those metal–metal bond lengths associated with Ru(3) as compared to Ru(1) and Ru(2). Metal–metal bonds associated with Ru(4) are similar to the Ru(1)–

(22) Beno, M. A.; Williams, J. M.; Tachikawa, M.; Muetterties, E. L. *J. Am. Chem. Soc.* **1981**, *103*, 1485.

Table II. Final Atomic Coordinates (×10⁴) and Equivalent Isotropic Displacement Coefficients (Å² × 10³) for (μ-H)Ru₄(μ₄-η²-COMe)(CO)₁₂

	x	y	z	U(eq)[a]
Ru(1)	4310 (1)	8440 (1)	3837 (1)	42 (1)
Ru(2)	1820 (1)	7686 (1)	3213 (1)	47 (1)
Ru(3)	3908 (1)	5653 (1)	3477 (1)	60 (1)
Ru(4)	1564 (1)	8820 (1)	4246 (1)	56 (1)
H(1)	3176 (77)	8955 (78)	3238 (29)	92 (24)
O(1)	2592 (7)	5777 (6)	4173 (2)	94 (2)
O(11)	5836 (6)	7767 (7)	4898 (2)	91 (2)
O(12)	4328 (7)	11662 (6)	3955 (2)	88 (2)
O(13)	7068 (6)	8518 (7)	3222 (2)	100 (3)
O(21)	−707 (7)	5659 (7)	3199 (3)	102 (3)
O(22)	2532 (8)	7419 (8)	2029 (2)	115 (3)
O(23)	−54 (7)	10305 (7)	2994 (2)	101 (3)
O(31)	2267 (8)	3109 (7)	3008 (3)	104 (3)
O(32)	6538 (8)	4326 (7)	4040 (3)	109 (3)
O(33)	5513 (8)	6032 (7)	2480 (3)	112 (3)
O(41)	2498 (6)	8977 (7)	5418 (2)	92 (2)
O(42)	−1351 (6)	7572 (8)	4454 (3)	107 (3)
O(43)	743 (10)	12000 (8)	4123 (3)	132 (4)
C(1)	2502 (8)	7145 (7)	4001 (3)	57 (2)
C(2)	2388 (18)	5236 (13)	4590 (5)	205 (9)
C(11)	5289 (7)	8009 (8)	4497 (3)	58 (3)
C(12)	4265 (8)	10449 (8)	3926 (3)	57 (3)
C(13)	6034 (8)	8445 (8)	3440 (3)	64 (3)
C(21)	241 (8)	6411 (9)	3196 (3)	65 (3)
C(22)	2251 (9)	7464 (9)	2456 (3)	77 (3)
C(23)	659 (8)	9355 (8)	3103 (3)	66 (3)
C(31)	2905 (10)	4026 (9)	3185 (3)	79 (3)
C(32)	5557 (10)	4795 (8)	3832 (3)	74 (3)
C(33)	4908 (10)	5896 (8)	2859 (4)	82 (4)
C(41)	2121 (8)	8945 (8)	4978 (3)	65 (3)
C(42)	−298 (9)	8080 (9)	4385 (3)	70 (3)
C(43)	1056 (10)	10888 (10)	4162 (3)	80 (3)

[a] Equivalent isotropic U defined as one-third of the trace of the orthogonalized U_{ij} tensor.

Table III. Final Atomic Coordinates (×10⁴) and Equivalent Isotropic Displacement Coefficients (Å² × 10³) for (μ-H)Ru₃Fe(μ₄-η²-COMe)(CO)₁₂

	x	y	z	U(eq)
Ru(1)	1819 (1)	2279 (1)	3226 (1)	46 (1)
Ru(2)	4318 (1)	1536 (1)	3846 (1)	41 (1)
Ru(3)	3895 (1)	4323 (1)	3500 (1)	58 (1)
Fe(1)	1595 (1)	1214 (1)	4253 (1)	44 (1)
H(1)	3198 (98)	1257 (97)	3316 (38)	98 (31)
O(1)	2601 (9)	4159 (7)	4215 (3)	90 (3)
O(11)	−727 (9)	4324 (9)	3200 (3)	102 (3)
O(12)	2575 (10)	2544 (10)	2039 (3)	110 (4)
O(13)	−61 (8)	−332 (9)	3000 (3)	100 (4)
O(21)	5855 (8)	2296 (9)	4900 (3)	94 (3)
O(22)	7080 (8)	1478 (9)	3207 (3)	97 (3)
O(23)	4393 (8)	−1691 (7)	3959 (3)	87 (3)
O(31)	6560 (10)	5631 (9)	4051 (4)	107 (4)
O(32)	2248 (10)	6864 (9)	3032 (3)	106 (4)
O(33)	5554 (10)	3986 (9)	2486 (3)	107 (4)
O(41)	−1284 (8)	2370 (9)	4443 (3)	102 (3)
O(42)	2480 (8)	1081 (9)	5383 (3)	91 (3)
O(43)	877 (11)	−1848 (9)	4134 (4)	113 (4)
C(1)	2472 (10)	2797 (9)	4029 (3)	54 (3)
C(2)	2070 (23)	4797 (14)	4559 (7)	220 (12)
C(11)	237 (11)	3577 (11)	3202 (4)	66 (4)
C(12)	2292 (11)	2505 (11)	2481 (4)	70 (4)
C(13)	645 (10)	614 (11)	3101 (4)	65 (4)
C(21)	5322 (9)	2012 (10)	4503 (4)	55 (3)
C(22)	6054 (10)	1538 (10)	3446 (4)	58 (3)
C(23)	4316 (10)	−497 (11)	3930 (4)	59 (4)
C(31)	5579 (12)	5179 (11)	3859 (5)	73 (4)
C(32)	2875 (12)	5947 (11)	3208 (4)	73 (4)
C(33)	4899 (12)	4101 (10)	2871 (5)	75 (4)
C(41)	−147 (11)	1874 (11)	4369 (4)	66 (4)
C(42)	2098 (10)	1097 (10)	4935 (5)	65 (4)
C(43)	1173 (11)	−688 (12)	4161 (4)	75 (4)

[a] Equivalent isotropic U defined as one-third of the trace of the orthogonalized U_{ij} tensor.

Ru(2) bond length. The interaction between Ru(3) and O(1) thus seems to shorten the metal–metal bond lengths. The fold angle, between the planes Ru(1)–Ru(3)–Ru(2) and Ru(1)–Ru(4)–Ru(2), is 120.8°.

The hydride ligand bridges atoms Ru(1) and Ru(2) with Ru(1)–H(1) = 1.86 (7) Å, Ru(2)–H(1) = 1.74 (7) Å, and Ru(1)–H(1)–Ru(2) = 103 (4)°. The Ru(1)–Ru(2) bond length is, as expected, the longest in the core due to the presence of the bridging hydride atom. Nevertheless this bond length is still shorter than would be expected for an unsupported Ru–H–Ru system.[23,24]

The tetraruthenium core is capped by a methoxyalkylidyne ligand in which ruthenium–carbon distances are Ru(1)–C(1) = 2.131 (7) Å, Ru(2)–C(1) = 2.110 (6) Å, Ru(3)–C(1) = 2.358 (7) Å, and Ru(4)–C(1) = 1.918 (7) Å. Angles of interest are Ru(1)–C(1)–Ru(3) = 77.0 (2)°, Ru(2)–C(1)–Ru(3) = 76.9 (2)°, Ru(1)–C(1)–Ru(4) = 87.7 (3)°, and Ru(2)–C(1)–Ru(4) = 88.7 (3)°. The carbon atom of the capping μ_4-η^2-COMe ligand is not linked symmetrically to all four ruthenium atoms. The bond Ru(4)–C(1) is far shorter and the Ru(3)–C(1) distance is much longer than the other Ru–C(1) distances. Ru(3) is also involved with an interaction to the oxygen atom of the methoxyalkylidyne ligand; the Ru(3)–O(1) distance is 2.175 (6) Å. The methoxy fragment of the methoxyalkylidyne ligand is bent away from Ru(4) with angles about C(1) of Ru(4)–C(1)–O(1) = 134.7 (5)°, Ru(3)–C(1)–O(1) = 65.3 (4)°, Ru(1)–C(1)–O(1) = 124.5 (5)°, Ru(2)–C(1)–O(1) = 122.4 (5)°, and Ru(3)–O(1)–C(2) = 143.1 (8)°. The equivalence of angles

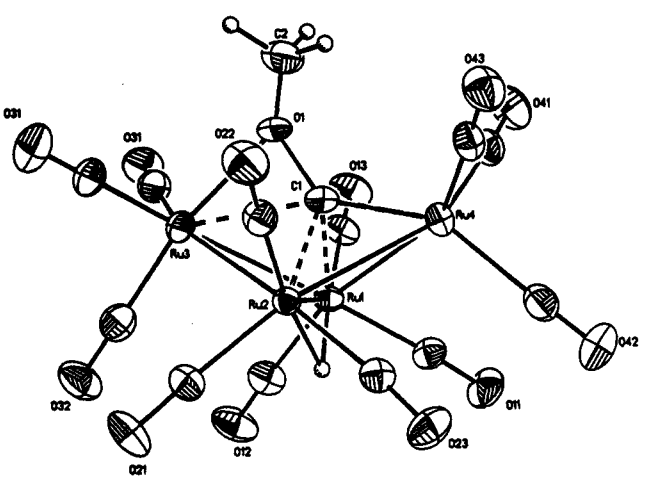

Figure 1. Labeling of atoms for (μ-H)Ru₄(μ₄-η²-COMe)(CO)₁₂ (ORTEP2 diagram).

Ru(1)–C(1)–O(1) and Ru(2)–C(1)–O(1) shows that the methoxy group lies in a pseudomirror plane containing Ru(3), Ru(4), and C(1) (Figure 2).

There are three terminal carbonyl ligands bonded to each ruthenium atom. These 12 carbonyl ligands have ruthenium–carbon bond distances ranging from 1.853 (10) to 2.017 (10) Å. There is no clear-cut pattern to the variations in Ru–CO bond lengths.

(μ-H)Ru₃Fe(μ₄-η²-COMe)(CO)₁₂. Reactions of sources of $Fe(CO)_x$ fragments with (μ-H)Ru₃(μ-CX)(CO)₁₀ (X = OMe, NMe_2) led to extremely low yields of the corresponding (μ-H)Ru₃Fe(μ₄-η²-CX)(CO)₁₂. The similarity of the chemical shifts of the hydride resonances in the Ru₄ and Ru₃Fe clusters is consistent with the hydride ligands

(23) Churchill, M. R.; DeBoer, B. G.; Rotella, F. J. *Inorg. Chem.* **1976**, *15*, 1843.
(24) Churchill, M. R. *Adv. Chem. Ser.* **1978**, *No. 167*, 36.

Table IV. Interatomic Distances (Å) for $(\mu\text{-H})Ru_4(\mu_4\text{-}\eta^2\text{-COMe})(CO)_{12}$

Ru(1)–Ru(2)	2.823 (1)	Ru(1)–Ru(3)	2.801 (1)
Ru(1)–Ru(4)	2.810 (1)	Ru(1)–C(1)	2.131 (7)
Ru(1)–C(11)	1.893 (7)	Ru(1)–C(12)	1.911 (7)
Ru(1)–C(13)	1.920 (8)	Ru(1)–H(1)	1.859 (71)
Ru(2)–Ru(3)	2.786 (1)	Ru(2)–Ru(4)	2.820 (1)
Ru(2)–C(1)	2.110 (6)	Ru(2)–C(21)	1.895 (8)
Ru(2)–C(22)	1.965 (9)	Ru(2)–C(23)	1.921 (8)
Ru(2)–H(1)	1.736 (71)	Ru(3)–O(1)	2.175 (6)
Ru(3)–C(1)	2.358 (7)	Ru(3)–C(31)	1.924 (9)
Ru(3)–C(32)	1.914 (8)	Ru(3)–C(33)	1.853 (10)
Ru(4)–C(1)	1.918 (7)	Ru(4)–C(41)	1.887 (8)
Ru(4)–C(42)	1.910 (8)	Ru(4)–C(43)	2.017 (10)
O(1)–C(1)	1.362 (9)	O(1)–C(2)	1.186 (14)
O(11)–C(11)	1.130 (9)	O(12)–C(12)	1.149 (9)
O(13)–C(13)	1.126 (10)	O(21)–C(21)	1.131 (10)
O(22)–C(22)	1.112 (11)	O(23)–C(23)	1.141 (10)
O(31)–C(31)	1.129 (11)	O(32)–C(32)	1.121 (11)
O(33)–C(33)	1.131 (12)	O(41)–C(41)	1.141 (10)
O(42)–C(42)	1.109 (10)	O(43)–C(43)	1.092 (12)

bridging two Ru atoms in each case. The low yields prevented complete characterization by spectroscopic methods.

The structure of $(\mu\text{-H})Ru_3Fe(\mu_4\text{-}\eta^2\text{-COMe})(CO)_{12}$ was determined by X-ray crystallography. The unit cell consists of four discrete molecular units separated by normal van der Waals distances. There are no anomalously short intermolecular distances. The labeling of atoms is shown in Figure 3. Selected interatomic distances and angles are collected in Tables VI and VII. The crystal is isomorphous with $(\mu\text{-H})Ru_4(\mu_4\text{-}\eta^2\text{-COMe})(CO)_{12}$.

The tetranuclear core consists of three ruthenium atoms and one iron atom which are arranged in a butterfly configuration with the iron atom (Fe(1)) occupying the wing-tip position corresponding to that of Ru(4) in the tetraruthenium cluster. The tetranuclear core had the following distances: Ru(1)–Ru(2) = 2.818 (1) Å, Ru(1)–Ru(3) = 2.783 (1) Å, Ru(2)–Ru(3) = 2.789 (1) Å, Ru(1)–Fe(1) = 2.751 (1) Å, and Ru(2)–Fe(1) = 2.740 (1) Å. Angles here are Ru(2)–Ru(1)–Ru(3) = 59.7°, Ru(2)–Ru(1)–Fe(1) = 58.9 (1)°, Ru(1)–Ru(2)–Ru(3) = 59.5 (1)°, Ru(1)–Ru(2)–Fe(1) = 59.3 (1)°, Ru(1)–Ru(3)–Ru(2) = 60.8 (1)°, and Ru(1)–Fe(1)–Ru(2) = 61.8 (1)°. These distances are similar to those of the tetraruthenium cluster with deviations caused by the smaller covalent radius of iron relative to ruthenium. The possibility of disorder of the iron atom in the core was examined in the light of the residual peaks of electron density near Fe(1). This was done by placing composite iron–ruthenium atoms at the four positions in the metal core and refining the coupled occupancies. None of the metal sites in the butterfly core showed any significant indications of disorder. Therefore, the iron atom occupies one specific position in the core. The angle of fold of the iron-substituted molecule is slightly smaller (118.7°) than the equivalent angle in the tetraruthenium cluster.

The iron-substituted cluster contains a bridging hydride ligand located in the same relative position as the hydride ligand in $(\mu\text{-H})Ru_4(\mu_4\text{-}\eta^2\text{-COMe})(CO)_{12}$. The distances and angle for the hydride ligand are Ru(1)–H(1) = 1.60 (9) Å, Ru(2)–H(1) = 1.67 (9) Å, and Ru(1)–H(1)–Ru(2) = 119 (5)°. The hydrido-bridged Ru(1)–Ru(2) linkage is the longest metal–metal bond in this cluster.

The core is capped by a methoxyalkylidyne ligand as in the tetraruthenium cluster. It is bonded to the metallic core with the distances Ru(1)–C(1) = 2.124 (8) Å, Ru(2)–C(1) = 2.131 (9) Å, Ru(3)–C(1) = 2.366 (8) Å, and Fe(1)–C(1) = 1.791 (8) Å. Angles of interest are Ru(1)–C(1)–Ru(3) = 76.4 (3) °, Ru(2)–C(1)–Ru(3) = 76.5 (3)°, Ru(1)–C(1)–Fe(1) = 88.9 (3)°, and Ru(2)–C(1)–Fe(1) = 88.2 (3)°. These dimensions follow the same trend as those for $(\mu\text{-H})Ru_4(\mu_4\text{-}\eta^2\text{-COMe})(CO)_{12}$. The methoxyalkylidyne ligand has its strongest interaction with Fe(1) (the site occupied by Ru(4) in the previous structure) and its weakest interaction with Ru(3). The carbon–oxygen bond in the COMe ligand is bent toward Ru(3) with angles of Ru(1)–C(1)–O(1) = 123.4 (6)°, Ru(2)–C(1)–O(1) = 122.3 (6)°, Ru(3)–C(1)–O(1) = 64.6 (4)°, Fe(1)–C(1)–O(1) = 135.6 (7)°, and Ru(3)–O(1)–C(2) = 144.5 (9)°. These angles are similar to those in the previous molecule. Atom O(1) is bonded to Ru(3) at a distance of 2.167 (8) Å. This

Table V. Bond Angles (deg) for $(\mu\text{-H})Ru_4(\mu_4\text{-}\eta^2\text{-COMe})(CO)_{12}$

Ru(2)–Ru(1)–Ru(3)	59.4 (1)	Ru(2)–Ru(1)–Ru(4)	60.1 (1)
Ru(3)–Ru(1)–Ru(4)	97.3 (1)	Ru(2)–Ru(1)–C(1)	47.9 (2)
Ru(3)–Ru(1)–C(1)	55.1 (2)	Ru(4)–Ru(1)–C(1)	43.0 (2)
Ru(2)–Ru(1)–C(11)	141.1 (2)	Ru(3)–Ru(1)–C(11)	97.5 (2)
Ru(4)–Ru(1)–C(11)	96.8 (2)	C(1)–Ru(1)–C(11)	93.4 (3)
Ru(2)–Ru(1)–C(12)	107.1 (2)	Ru(3)–Ru(1)–C(12)	165.2 (2)
Ru(4)–Ru(1)–C(12)	78.8 (2)	C(1)–Ru(1)–C(12)	121.7 (3)
C(11)–Ru(1)–C(12)	97.1 (3)	RU(2)–Ru(1)–C(13)	113.2 (2)
Ru(3)–Ru(1)–C(13)	86.4 (2)	Ru(4)–Ru(1)–C(13)	167.8 (2)
C(1)–Ru(1)–C(13)	141.5 (3)	C(11)–Ru(1)–C(13)	94.2 (3)
C(12)–Ru(1)–C(13)	94.6 (3)	Ru(2)–Ru(1)–H(1)	36.7 (22)
Ru(3)–Ru(1)–H(1)	85.6 (23)	Ru(4)–Ru(1)–H(1)	76.7 (22)
C(1)–Ru(1)–H(1)	83.3 (22)	C(11)–Ru(1)–H(1)	173.1 (22)
C(12)–Ru(1)–H(1)	79.6 (23)	C(13)–Ru(1)–H(1)	92.1 (22)
Ru(1)–Ru(2)–Ru(3)	59.9 (1)	Ru(1)–Ru(2)–Ru(4)	59.7 (1)
Ru(3)–Ru(2)–Ru(4)	97.4 (1)	Ru(1)–Ru(2)–C(1)	48.6 (2)
Ru(3)–Ru(2)–C(1)	55.5 (2)	Ru(4)–Ru(2)–C(1)	42.9 (2)
Ru(1)–Ru(2)–C(21)	141.8 (2)	Ru(3)–Ru(2)–C(21)	95.5 (2)
Ru(4)–Ru(2)–C(21)	99.5 (2)	C(1)–Ru(2)–C(21)	93.8 (3)
Ru(1)–Ru(2)–C(22)	111.4 (2)	Ru(3)–Ru(2)–C(22)	89.3 (2)
Ru(4)–Ru(2)–C(22)	162.6 (2)	C(1)–Ru(2)–C(22)	144.3 (3)
C(21)–Ru(2)–C(22)	95.8 (3)	Ru(1)–Ru(2)–C(23)	108.2 (2)
Ru(3)–Ru(2)–C(23)	168.1 (2)	Ru(4)–Ru(2)–C(23)	75.5 (2)
C(1)–Ru(2)–C(23)	118.3 (3)	C(21)–Ru(2)–C(23)	95.1 (3)
C(22)–Ru(2)–C(23)	95.0 (3)	Ru(1)–Ru(2)–H(1)	39.8 (24)
Ru(3)–Ru(2)–H(1)	88.4 (25)	Ru(4)–Ru(2)–H(1)	78.1 (24)
C(1)–Ru(2)–H(1)	86.9 (24)	C(21)–Ru(2)–H(1)	175.7 (24)
C(22)–Ru(2)–H(1)	86.0 (24)	C(23)–Ru(2)–H(1)	80.8 (25)
Ru(1)–Ru(3)–Ru(2)	60.7 (1)	Ru(1)–Ru(3)–O(1)	76.3 (1)
Ru(2)–Ru(3)–O(1)	75.2 (2)	Ru(1)–Ru(3)–C(1)	47.8 (2)
Ru(2)–Ru(3)–C(1)	47.5 (2)	O(1)–Ru(3)–C(1)	34.7 (2)
Ru(1)–Ru(3)–C(31)	158.1 (3)	Ru(2)–Ru(3)–C(31)	98.1 (3)
O(1)–Ru(3)–C(31)	93.9 (3)	C(1)–Ru(3)–C(31)	114.7 (3)
Ru(1)–Ru(3)–C(32)	99.0 (2)	Ru(2)–Ru(3)–C(32)	159.2 (2)
O(1)–Ru(3)–C(32)	96.7 (3)	C(1)–Ru(3)–C(32)	116.4 (3)
C(31)–Ru(3)–C(32)	101.6 (3)	Ru(1)–Ru(3)–C(33)	95.1 (2)
Ru(2)–Ru(3)–C(33)	94.9 (3)	O(1)–Ru(3)–C(33)	169.1 (3)
C(1)–Ru(3)–C(33)	134.5 (3)	C(31)–Ru(3)–C(33)	91.9 (4)
C(32)–Ru(3)–C(33)	91.2 (4)	Ru(1)–Ru(4)–Ru(2)	60.2 (1)
Ru(1)–Ru(4)–C(1)	49.3 (2)	Ru(2)–Ru(4)–C(1)	48.4 (2)
Ru(1)–Ru(4)–C(41)	98.5 (2)	Ru(2)–Ru(4)–C(41)	152.2 (2)
C(1)–Ru(4)–C(41)	104.7 (3)	Ru(1)–Ru(4)–C(42)	149.5 (3)
Ru(2)–Ru(4)–C(42)	98.2 (2)	C(1)–Ru(4)–C(42)	100.5 (3)
C(41)–Ru(4)–C(42)	93.2 (3)	Ru(1)–Ru(4)–C(43)	107.3 (3)
Ru(2)–Ru(4)–C(43)	107.5 (2)	C(1)–Ru(4)–C(43)	150.7 (3)
C(41)–Ru(4)–C(43)	95.4 (3)	C(42)–Ru(4)–C(43)	99.5 (4)
Ru(3)–O(1)–C(1)	80.1 (4)	Ru(3)–O(1)–C(2)	143.1 (8)
C(1)–O(1)–C(2)	132.5 (8)	Ru(1)–C(1)–Ru(2)	83.5 (2)
Ru(1)–C(1)–Ru(3)	77.0 (2)	Ru(2)–C(1)–Ru(3)	76.9 (2)
Ru(1)–C(1)–Ru(4)	87.7 (3)	Ru(2)–C(1)–Ru(4)	88.7 (3)
Ru(3)–C(1)–Ru(4)	160.0 (4)	Ru(1)–C(1)–O(1)	124.5 (5)
Ru(2)–C(1)–O(1)	122.4 (5)	Ru(3)–C(1)–O(1)	65.3 (4)
Ru(4)–C(1)–O(1)	134.7 (5)	Ru(1)–C(11)–O(11)	177.8 (6)
Ru(1)–C(12)–O(12)	174.7 (6)	Ru(1)–C(13)–O(13)	176.0 (7)
Ru(2)–C(21)–O(21)	178.2 (7)	Ru(2)–C(22)–O(22)	175.7 (8)
Ru(2)–C(23)–O(23)	174.0 (7)	Ru(3)–C(31)–O(31)	177.0 (8)
Ru(3)–C(32)–O(32)	178.2 (7)	Ru(3)–C(33)–O(33)	179.4 (5)
Ru(4)–C(41)–O(41)	177.2 (7)	Ru(4)–C(42)–O(42)	175.7 (8)
Ru(4)–C(43)–O(43)	177.9 (9)	Ru(1)–H(1)–Ru(2)	103.4 (37)

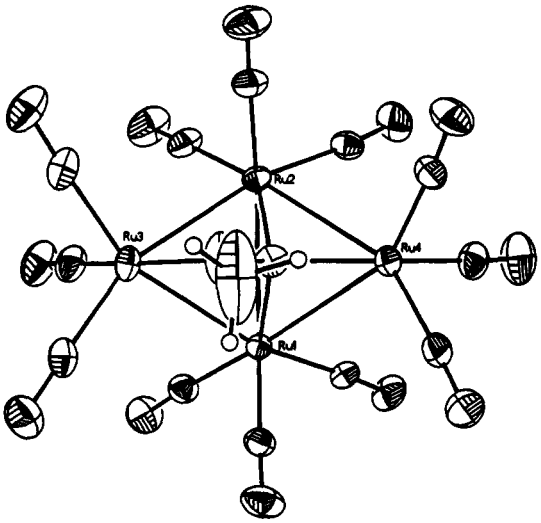

Figure 2. $(\mu\text{-H})Ru_4(\mu_4\text{-}\eta^2\text{-COMe})(CO)_{12}$ molecule, showing the orientation of the $\mu_4\text{-}\eta^2$-COMe ligand above the Ru_4 cluster (ORTEP2 diagram).

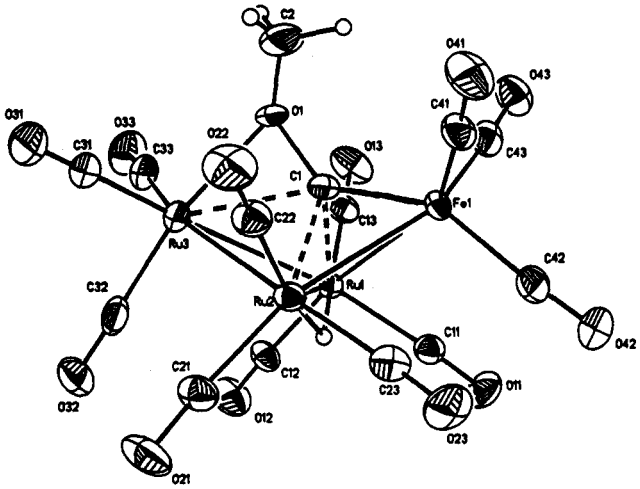

Figure 3. Labeling of atoms for $(\mu\text{-H})Ru_3Fe(\mu_4\text{-}\eta^2\text{-COMe})(CO)_{12}$ (ORTEP2 diagram).

Table VI. Interatomic Distances (Å) for $(\mu\text{-H})Ru_3Fe(\mu_4\text{-}\eta^2\text{-COMe})(CO)_{12}$

Ru(1)–Ru(2)	2.818 (1)	Ru(1)–Ru(3)	2.783 (1)
Ru(1)–Fe(1)	2.751 (1)	Ru(1)–C(1)	2.124 (8)
Ru(1)–C(11)	1.900 (10)	Ru(1)–C(12)	1.925 (10)
Ru(1)–C(13)	1.926 (10)	Ru(1)–H(1)	1.603 (90)
Ru(2)–Ru(3)	2.789 (1)	Ru(2)–Fe(1)	2.740 (1)
Ru(2)–C(1)	2.131 (9)	Ru(2)–C(21)	1.906 (9)
Ru(2)–C(22)	1.901 (9)	Ru(2)–C(23)	1.930 (10)
Ru(2)–H(1)	1.670 (93)	Ru(3)–O(1)	2.167 (8)
Ru(3)–C(1)	2.366 (8)	Ru(3)–C(31)	1.942 (11)
Ru(3)–C(32)	1.927 (11)	Ru(3)–C(33)	1.847 (12)
Fe(1)–C(1)	1.791 (8)	Fe(1)–C(41)	1.749 (10)
Fe(1)–C(42)	1.748 (11)	Fe(1)–C(43)	1.848 (11)
O(1)–C(1)	1.369 (10)	O(1)–C(2)	1.162 (18)
O(11)–C(11)	1.132 (13)	O(12)–C(12)	1.134 (12)
O(13)–C(13)	1.128 (13)	O(21)–C(21)	1.123 (11)
O(22)–C(22)	1.128 (12)	O(23)–C(23)	1.131 (12)
O(31)–C(31)	1.095 (14)	O(32)–C(32)	1.122 (13)
O(33)–C(33)	1.146 (15)	O(41)–C(41)	1.163 (13)
O(42)–C(42)	1.156 (14)	O(43)–C(43)	1.129 (14)

ruthenium–oxygen distance is substantially shorter then the Ru(3)–C(1) distance of 2.366 (8) Å.

The 12 carbonyl ligands are arranged about the core so that each metal atom is associated with three terminally bonded carbonyl ligands. The ruthenium–carbon bond distances range from 1.847 (12) to 1.942 (11) Å, while iron–carbon distances range from 1.748 (11) to 1.848 (11) Å.

Table VII. Bond Angles (deg) for $(\mu\text{-H})Ru_3Fe(\mu_4\text{-}\eta^2\text{-COMe})(CO)_{12}$

Ru(2)–Ru(1)–Ru(3)	59.7 (1)	Ru(2)–Ru(1)–Fe(1)	58.9 (1)
Ru(3)–Ru(1)–Fe(1)	95.4 (1)	Ru(2)–Ru(1)–C(1)	48.6 (2)
Ru(3)–Ru(1)–C(1)	55.7 (2)	Fe(1)–Ru(1)–C(1)	40.6 (2)
Ru(2)–Ru(1)–C(11)	142.1 (3)	Ru(3)–Ru(1)–C(11)	94.6 (3)
Fe(1)–Ru(1)–C(11)	100.9 (3)	C(1)–Ru(1)–C(11)	94.5 (4)
Ru(2)–Ru(1)–C(12)	110.5 (3)	Ru(3)–Ru(1)–C(12)	89.3 (3)
Fe(1)–Ru(1)–C(12)	162.8 (3)	C(1)–Ru(1)–C(12)	144.3 (4)
C(11)–Ru(1)–C(12)	95.2 (4)	Ru(2)–Ru(1)–C(13)	109.3 (3)
Ru(3)–Ru(1)–C(13)	169.0 (3)	Fe(1)–Ru(1)–C(13)	78.3 (3)
C(1)–Ru(1)–C(13)	118.8 (4)	C(11)–Ru(1)–C(13)	95.5 (4)
C(12)–Ru(1)–C(13)	94.3 (4)	Ru(2)–Ru(1)–H(1)	31.3 (34)
Ru(3)–Ru(1)–H(1)	81.3 (32)	Fe(1)–Ru(1)–H(1)	74.4 (34)
C(1)–Ru(1)–H(1)	78.8 (33)	C(11)–Ru(1)–H(1)	173.3 (29)
C(12)–Ru(1)–H(1)	90.1 (34)	C(13)–Ru(1)–H(1)	88.2 (32)
Ru(1)–Ru(2)–Ru(3)	59.5 (1)	Ru(1)–Ru(2)–Fe(1)	59.3 (1)
Ru(3)–Ru(2)–Fe(1)	95.6 (1)	Ru(1)–Ru(2)–C(1)	48.4 (2)
Ru(3)–Ru(2)–C(1)	55.6 (2)	Fe(1)–Ru(2)–C(1)	40.8 (2)
Ru(1)–Ru(2)–C(21)	141.0 (3)	Ru(3)–Ru(2)–C(21)	95.8 (3)
Fe(1)–Ru(2)–C(21)	97.9 (3)	C(1)–Ru(2)–C(21)	93.2 (3)
Ru(1)–Ru(2)–C(22)	113.5 (3)	Ru(3)–Ru(2)–C(22)	87.2 (3)
Fe(1)–Ru(2)–C(22)	168.4 (3)	C(1)–Ru(2)–C(22)	142.7 (4)
C(21)–Ru(2)–C(22)	93.0 (4)	Ru(1)–Ru(2)–C(23)	107.7 (3)
Ru(3)–Ru(2)–C(23)	165.9 (3)	Fe(1)–Ru(2)–C(23)	81.1 (3)
C(1)–Ru(2)–C(23)	121.9 (4)	C(21)–Ru(2)–C(23)	98.2 (4)
C(22)–Ru(2)–C(23)	93.5 (4)	Ru(1)–Ru(2)–H(1)	29.9 (31)
Ru(3)–Ru(2)–H(1)	80.1 (31)	Fe(1)–Ru(2)–H(1)	73.9 (31)
C(1)–Ru(2)–H(1)	77.2 (31)	C(21)–Ru(2)–H(1)	170.3 (29)
C(22)–Ru(2)–H(1)	95.6 (31)	C(23)–Ru(2)–H(1)	85.8 (31)
Ru(1)–Ru(3)–Ru(2)	60.8 (1)	Ru(1)–Ru(3)–O(1)	76.3 (2)
Ru(2)–Ru(3)–O(1)	75.9 (2)	Ru(1)–Ru(3)–C(1)	47.9 (2)
Ru(2)–Ru(3)–C(1)	48.0 (2)	O(1)–Ru(3)–C(1)	34.8 (3)
Ru(1)–Ru(3)–C(31)	158.9 (3)	Ru(2)–Ru(3)–C(31)	98.5 (3)
O(1)–Ru(3)–C(31)	95.8 (4)	C(1)–Ru(3)–C(31)	116.3 (4)
Ru(1)–Ru(3)–C(32)	97.8 (3)	Ru(2)–Ru(3)–C(32)	158.0 (3)
O(1)–Ru(3)–C(32)	95.3 (4)	C(1)–Ru(3)–C(32)	115.0 (4)
C(31)–Ru(3)–C(32)	102.5 (4)	Ru(1)–Ru(3)–C(33)	94.0 (3)
Ru(2)–Ru(3)–C(33)	94.9 (3)	O(1)–Ru(3)–C(33)	168.9 (3)
C(1)–Ru(3)–C(33)	134.2 (3)	C(31)–Ru(3)–C(33)	91.5 (5)
C(32)–Ru(3)–C(33)	91.2 (4)	Ru(1)–Fe(1)–Ru(2)	61.8 (1)
Ru(1)–Fe(1)–C(1)	50.5 (3)	Ru(2)–Fe(1)–C(1)	51.0 (3)
Ru(1)–Fe(1)–C(41)	96.5 (3)	Ru(2)–Fe(1)–C(41)	150.5 (3)
C(1)–Fe(1)–C(41)	100.1 (4)	Ru(1)–Fe(1)–C(42)	153.7 (3)
Ru(2)–Fe(1)–C(42)	98.3 (3)	C(1)–Fe(1)–C(42)	104.1 (4)
C(41)–Fe(1)–C(42)	94.7 (4)	Ru(1)–Fe(1)–C(43)	105.1 (3)
Ru(2)–Fe(1)–C(43)	104.6 (3)	C(1)–Fe(1)–C(43)	149.9 (4)
C(41)–Fe(1)–C(43)	100.1 (5)	C(42)–Fe(1)–C(43)	96.2 (5)
Ru(3)–O(1)–C(1)	80.6 (5)	Ru(3)–O(1)–C(2)	144.5 (9)
C(1)–O(1)–C(2)	134.3 (11)	Ru(1)–C(1)–Ru(2)	83.0 (3)
Ru(1)–C(1)–Ru(3)	76.4 (3)	Ru(2)–C(1)–Ru(3)	76.5 (3)
Ru(1)–C(1)–Fe(1)	88.9 (3)	Ru(2)–C(1)–Fe(1)	88.2 (3)
Ru(3)–C(1)–Fe(1)	159.8 (5)	Ru(1)–C(1)–O(1)	123.4 (6)
Ru(2)–C(1)–O(1)	122.3 (6)	Ru(3)–C(1)–O(1)	64.6 (4)
Fe(1)–C(1)–O(1)	135.6 (7)	Ru(1)–C(11)–O(11)	177.7 (9)
Ru(1)–C(12)–O(12)	175.5 (9)	Ru(1)–C(13)–O(13)	176.2 (9)
Ru(2)–C(21)–O(21)	176.9 (8)	Ru(2)–C(22)–O(22)	177.1 (9)
Ru(2)–C(23)–O(23)	175.4 (8)	Ru(3)–C(31)–O(31)	177.5 (9)
Ru(3)–C(32)–O(32)	177.8 (9)	Ru(3)–C(33)–O(33)	178.0 (10)
Fe(1)–C(41)–O(41)	177.1 (9)	Fe(1)–C(42)–O(42)	176.3 (9)
Fe(1)–C(43)–O(43)	175.9 (10)	Ru(1)–H(1)–Ru(2)	118.8 (56)

Comparison of $(\mu\text{-H})M_4(\mu_4\text{-}\eta^2\text{-CX})(CO)_{12}$ Structures. It is remarkable that the dimensions of the M_4C core are so insensitive to the metal composition and alkylidyne substituent (Table VIII). Other than the shorter bond distances to iron, as expected from the smaller covalent radius, there are no significant differences in the M_4C core parameters. Comparison of $(\mu\text{-H})Ru_3M(\mu_4\text{-}\eta^2\text{-COMe})(CO)_{12}$, M = Fe_4, $FeRu_3$, and Ru_4, shows that the C–OMe bond is longest for the Fe_4 cluster. The structure provides no direct evidence for the preferred bonding of the oxygen atom to ruthenium rather than iron in the mixed-metal cluster.

Table VIII. Comparison of Structural Parameters for $(\mu\text{-H})M_4(\mu_4\text{-}\eta^2\text{-CX})(CO)_{12}$ (X = OMe, M_4 = Fe_4, Ru_3Fe, Ru_4; X = NMe_2, M_4 = Ru_4)

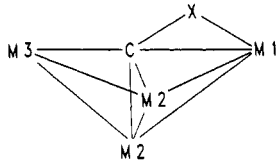

X	M_4	M1–C, Å	M3–C, Å	M2–C, Å	M1–M2–M3, deg	C–X, Å	M1–X, Å	M1–C–M3, deg
OMe	Ru_4	2.358 (7)	1.918 (7)	2.110 (6)	97.4 (1)	1.362 (9)	2.175 (6)	160.0 (4)
				2.131 (7)	97.3 (1)			
OMe	Ru_3Fe	2.366 (8)	1.791 (8)	2.124 (8)	95.4 (1)	1.369 (10)	2.167 (8)	159.8 (5)
				2.131 (9)	95.6 (1)			
OMe[a]	Fe_4	2.137 (2)	1.834 (2)	1.948 (2)	97.42 (3)	1.398 (2)	2.000 (2)	162.4
				1.972 (2)	96.19 (2)			
NMe_2[b]	Ru_4	2.316 (5)	1.964 (5)	2.146 (5)	96.31 (2)	1.434 (6)	2.149 (4)	159.4 (2)
				2.161 (5)	96.77 (2)			

[a] See ref 2d. [b] See ref 7.

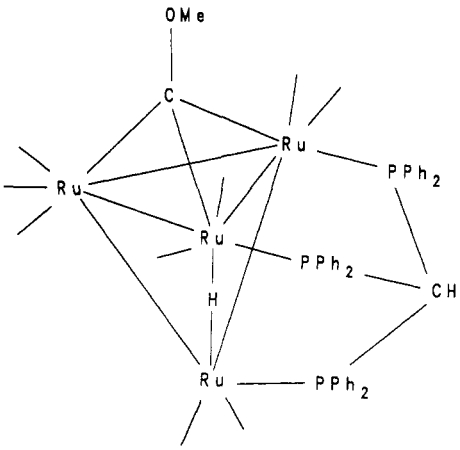

Figure 4. Proposed structure for $(\mu\text{-H})Ru_4(\mu_3\text{-COMe})(CO)_9\{(PPh_2)_3CH\}$.

$(\mu$-H)$Ru_4(\mu_3$-COMe)$(CO)_9\{\mu_3$-$(PPh_2)_3CH\}$. A second approach to the synthesis of tetrametallic alkylidynes was provided by our synthesis of $(\mu\text{-H})_3Ru_3(\mu_3\text{-COMe})(CO)_7\{\mu_2\text{-}(PPh_2)_2CHPPh_2\}$. The $(PPh_2)_3CH$ ligand cannot span the Ru_3 face of the triangular cluster but can do so for Ru_4 clusters.[12] Therefore, we thought that the pendant PPh_2 group of $(\mu\text{-H})_3Ru_3(\mu_3\text{-COMe})(CO)_7\{\mu_2\text{-}(PPh_2)_2CHPPh_2\}$ might provide a tether to introduce a fourth metal atom.

Reaction of $Ru(CO)_4(C_2H_4)$ with $(\mu\text{-H})_3Ru_3(\mu_3\text{-COMe})(CO)_7\{\mu_2\text{-}(PPh_2)_2CHPPh_2\}$ yielded $(\mu\text{-H})Ru_4(COMe)(CO)_9\{(PPh_2)_3CH\}$ (27% yield). This product was characterized by mass spectroscopy and by ^1H, ^{13}C, and ^{31}P NMR and IR spectroscopy. The composition is indicated by the molecular ion in the mass spectrum.[14] The product decomposes slowly in solution or in the solid state even at −20 °C, and crystals suitable for an X-ray diffraction study have not been obtained.[25]

The proposed structure is shown in Figure 4. The ^{31}P NMR spectrum at low temperature consists of three resonances due to Ru-coordinated phosphorus atoms; two

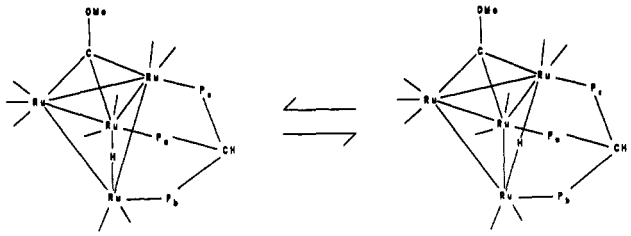

Figure 5. Proposed fluxional process for $(\mu\text{-H})Ru_4(\mu_3\text{-COMe})(CO)_9\{(PPh_2)_3CH\}$.

of these resonances broaden and collapse into a single resonance above room temperature. However, the ^1H NMR resonance for the single hydride at room temperature displays equivalent coupling constants to three ^{31}P nuclei, in addition to coupling to the CH proton. This suggests that hydride fluxionality, as shown in Figure 5, between two Ru–Ru edges renders two of the three phosphorus atoms equivalent and that the third phosphorus–hydride coupling constant is coincidentally equal to the average for the first two. Line-shape calculations for the ^{31}P spectrum indicate a rate constant of ca. 10^5 s^{-1} at 22 °C ($\Delta G^\ddagger$ = 40 kJ/mol), a value consistent with hydride fluxionality.[27] At −90 °C the hydride resonance is very broad and featureless, due either to unresolved coupling in a more complicated multiplet (e.g., dddd) or to exchange. A plausible description can be made by assuming J_{HH} of 2 Hz and J_{PH} of 26, 13, and 0 Hz between the hydride and P_a, P_b, and P_c, respectively (Figure 5); fluxional averaging of P_a and P_c would give rise to the observed fast-exchange hydride spectrum. Although the coincidence of the coupling to P_b and the average of the couplings to P_a and P_c is a somewhat unsatisfying explanation for the quartet hydride pattern at room temperature, the values of the hydride–phosphorus coupling constants are consistent with those found in other clusters. Values for cis P–μ-H coupling constants range from 6 Hz (e.g. $(\mu\text{-H})Ru_3(\mu\text{-CNMeBz})(CO)_9(PPh_3)$[27]) to 22 Hz (e.g. $(\mu\text{-H})_3Ru_3(\mu_3\text{-COMe})(CO)_6\{(PPh_2CH_2)_3CMe\}$[12]).

The ^{13}C NMR spectrum is most consistent with a capped tetrahedral structure (type I). The resonance attributed to the alkylidyne carbon, 350.5 ppm, is similar to those of related type I tetrahedral $Fe_4(CR)$ clusters and quite different from the shifts found for type III clusters.[21]

(25) Although lovely brown-red needles were obtained by recrystallization from methanol/dichloromethane, these were too small for X-ray analysis, and elemental analysis consistentily was low in carbon content, although within range for hydrogen. We attribute the low carbon analysis to CO loss in transit (the compound decomposes slowly even at −20 °C in the solid state) or to incomplete combustion (low carbon analyses have been reported for some, but not all, cluster complexes of the $(PPh_2)_3CH$ ligand).

(26) Dalton, D. M.; Barnett, D. J.; Duggan, T. P.; Keister, J. B.; Malik, P. T.; Modi, S. P.; Shaffer, M. R.; Smesko, S. A. *Organometallics* **1985**, *4*, 1854.

(27) Nevinger, L. R.; Keister, J. B. *Organometallics* **1990**, *9*, 2312 and references therein.

(28) Cowie, A. G.; Johnson, B. F. G.; Lewis, J.; Raithby, P. R. *J. Organomet. Chem.* **1986**, *306*, C63.

Equivalent coupling (19 Hz) of the methylidyne carbon resonance to two ^{31}P nuclei is observed, suggesting that the COMe ligand bridges between two phosphorus-substituted Ru atoms. The 3:2:2:2 carbonyl pattern is consistent with the process shown in Figure 5 if 3-fold fluxional exchange makes the $Ru(CO)_3$ resonances broad. The small quantity of the cluster available and decomposition in solution precluded the acquisition of low-temperature spectra.

Conclusions. We have prepared new tetraruthenium clusters containing μ_4-η^2-COMe and μ_3-η^1-COMe ligands. These clusters are unstable with respect to fragmentation, seemingly more so than the tetrairon analogs. Crystallographic characterizations of $(\mu\text{-H})Ru_3M(\mu_4\text{-}\eta^2\text{-COMe})(CO)_{12}$ (M = Ru, Fe) indicate preferential coordination of the OMe group to the wing-tip Ru atom rather than the wing-tip Fe atom.

Acknowledgment. This work was supported by the National Science Foundation through Grant CHE8900921. We thank Professor R. D. Adams of the University of South Carolina for helpful discussions. Purchase of the Siemens R3m/V diffractometer was made possible by Grant 89-13733 from the Chemical Instrumentation Program of the National Science Foundation.

Supplementary Material Available: Tables of anisotropic thermal parameters and calculated hydrogen atom positions for $(\mu\text{-H})Ru_4(\mu_4\text{-}\eta^2\text{-COMe})(CO)_{12}$ and $(\mu\text{-H})Ru_3Fe(\mu_4\text{-}\eta^2\text{-COMe})(CO)_{12}$ (2 pages). Ordering information is given on any current masthead page.

OM920336K